Formononetin, an isoflavone, relaxes rat isolated aorta through endothelium-dependent and endothelium-independent pathways

Jian-Hong Wu[1], Qing Li[1,2], Min-Yi Wu[1], De-Jian Guo[1], Huan-Le Chen[1], Shi-Lin Chen[1,2], Sai-Wang Seto[3], Alice L.S. Au[3], Christina C.W. Poon[3], George P.H. Leung[4], Simon M.Y. Lee[5], Yiu-Wa Kwan[3], Shun-Wan Chan[1,6,*]

[1] State Key Laboratory of Chinese Medicine and Molecular Pharmacology, Shenzhen, PR China

[2] Institute of Medicinal Plant Development, Peking Union Medical College and Chinese Academy of Medical Sciences, Beijing, PR China

[3] Department of Pharmacology, Faculty of Medicine, The Chinese University of Hong Kong, Hong Kong SAR, PR China

[4] Department of Pharmacology, Faculty of Medicine, The University of Hong Kong, Hong Kong SAR, PR China

[5] Institute of Chinese Medical Sciences, University of Macau, Av. Padre Tomas Pereira S.J., Taipa, Macau, PR China

[6] Open Laboratory of Chirotechnology, Department of Applied Biology and Chemical Technology, The Hong Kong Polytechnic University, Hong Kong SAR, PR China

[*] Author for correspondence
Dr. Shun-Wan Chan
Open Laboratory of Chirotechnology
Department of Applied Biology and Chemical Technology
The Hong Kong Polytechnic University
Hong Kong SAR
PR China
Tel.: +852-34008718
Fax: +852-23649932
E-mail address: bcswchan@polyu.edu.hk

Abstract

We evaluated the vasorelaxation effects of formononetin, an isoflavone/phytoestrogen found abundantly in *Astragalus mongholicus* Bunge, on rat isolated aorta and the underlying mechanisms involved. Cumulative administration of formononetin, genistein, daidzein and biochanin A relaxed phenylephrine-preconstricted aorta. Formononetin and biochanin A caused a similar magnitude of relaxation whereas daidzein was least potent. Mechanical removal of endothelium, L-NAME (100 μM) and methylene blue (10 μM) suppressed formononetin-induced relaxation. Formononetin increased endothelial nitric oxide synthase (eNOS), but not iNOS, activity with an up-regulation of eNOS mRNA and p-eNOS^{Ser1177} protein expression. In endothelium-denuded preparations, formononetin-induced vasorelaxation was significantly reduced by glibenclamide (3 μM) and iberiotoxin (100 nM), and a combination of glibenclamide (3 μM) plus iberiotoxin (100 nM) abolished the relaxation. In contrast, formononetin-elicited endothelium-independent relaxation was not altered by ICI 182,780 (10 μM, an estrogen receptors (ERα/ERβ) antagonist) or mifepristone (10 μM, a progesterone receptor antagonist). In single aortic smooth muscle cells, formononetin caused opening of iberiotoxin-sensitive Ca^{2+}-activated K^+ (BK_{Ca}) channels and glibenclamide-sensitive ATP-dependent K^+ (K_{ATP}) channels. Thus, our results suggest that formononetin caused vascular relaxation via endothelium/NO-dependent mechanism and endothelium-independent mechanism which involves the activation of BK_{Ca} and K_{ATP} channels.

Keywords: Formononetin; nitric oxide; vasorelaxation; BK_{Ca} and K_{ATP} channels

1. Introduction

Cardiovascular disease is a major cause of death or disability in many developed countries. Smoking, high cholesterol and obesity are well known risk factors of cardiovascular disease, and they are associated with decreased availability of endothelial cells-derived NO in the cardiovascular system. Isoflavones are phytoestrogens that have been gathering an increased interest in the areas of clinical nutrition and diseases prevention [1,2] especially for post-menopausal women in view of the some unfavorable consequences/potential risks (e.g. stroke and coronary heart disease) associated with the use of estrogen-like substances (so-called hormone replacement therapy) [3]. Thus, there is an urgent need for estrogen alternatives (e.g. phytoestrogens) for providing beneficial cardiovascular effects. Recent studies provided evidence that isoflavones can restore endothelial dysfunction via an increase of NO generation [4–8].

Formononetin (7-hydroxy-3(4-methoxypheny)chromone ($C_{16}H_{12}O_4$) (Fig. 1)) is a isoflavonoid found abundantly in Traditional Chinese Medicine *Astragalus mongholicus* Bunge (known as Huang Qi in China and Ougi in Japan) and *Trifolium pratense* L (red clover) which belongs to the family *Leguminosae*. The extract of these herbs has been used clinically to treat different diseases including cardiovascular diseases in China for a long time [9–11]. In addition, formononetin possesses hypolipidemic properties [12], mammary gland proliferation function [13], anti-oxidative and estrogenic effects [14]. The extract of *Astragalus membraneaceus*

has also been demonstrated to possess endothelium-dependent and -independent vasodilatory effects [15–17] and daidzein, a metabolite of formononetin formed *in vivo*, can relax rats' aorta and pulmonary artery [18–20]. However, the underlying mechanisms of formononetin involved (especially its effects on ion channels modulation) in eliciting vasorelaxation has not been elucidated in details. Thus, in this study, we tested the hypothesis that formononetin-induced vascular relaxation involved the openings of K^+ channels of the vascular smooth muscle. More importantly, as formononetin is a phytoestrogen which shares a chemical structure similar to estrogen/progesterone (Fig. 1), the participation of estrogen and progesterone receptors in mediating the vascular responses will be elucidated.

2. Materials and methods

2.1. Drugs and chemicals

Formononetin was purchased from Acros Organics (Belgium) and the stock solution (100 mM) of formononetin was prepared in dimethyl sulphoxide and stored at -20 °C until use. Genistein, daidzein, biochanin A, phenylephrine hydrochloride, acetylcholine hydrochloride (ACh), neostigmine hydrobromide, indomethacin, N^{ω}-nitro-L-arginine methyl ester (L-NAME), methylene blue (MB), proporanolol and prazosin were obtained from Sigma-Aldrich (USA). 1400W, ICI 182,780, mifepristone, iberiotoxin and glibenclamide were purchased from Tocris Bioscience (UK). Kits for the determination of nitric oxide (NO) levels, endothelial NO synthase (eNOS), inducible NOS (iNOS) were provided by Nanjing Jiancheng Bioengineering Company (PR China). Other chemicals used were analytical grade.

2.2. Arterial rings preparation

Male Sprague-Dawley rats (~250-300 g) were killed by cervical dislocation, and thoracic aortas were dissected from animals immediately. The thoracic aortas were cleared from connective tissues and cut into rings (3 mm in length) and immersed in Krebs' solution of the following composition (mM): NaCl 118, KCl 4.7, $MgSO_4$ 1.2, KH_2PO_4 1.2, $NaHCO_3$ 25, glucose 11 and $CaCl_2$ 1.8 (pH 7.4). Care was taken not to

touch the lumen of the thoracic aortas during dissection to ensure the endothelium intact, unless otherwise stated. The thoracic aortic rings were immersed in a 5 mL glass (water-jacketed) tissue baths containing Krebs' solution (37 ± 1 °C) aerated continuously with a gas mixture of 95% O_2 and 5% CO_2 (pH 7.4; 37 ± 1 °C). The thoracic aortic rings were mounted on L-shaped metal prongs, which were connected to a force displacement MLT1030/D transducer (AD Instruments, Australia) coupled to the data acquisition programme (PowerLab 8SP, AD Instruments, Australia) for continuous recording of isometric tension changes. An optimal load of 10 ± 1 mN (determined from our preliminary studies) was applied progressively (2 mN per min) to aortic rings. Then, tissues were allowed to equilibrate for 60 min under the optimal resting tension. During the equilibration period, tissues were washed with drug-free Krebs' solution every 15 min and the resting tension was readjusted, if necessary, before commencing the experiments. After equilibration, the integrity of the aortic rings was confirmed with high K^+ (65 mM) until two consecutive contractile responses were reproducible. To exclude the involvement of cyclo-oxygenase cascade, indomethacin (1 μM, a non-selective cyclo-oxygenase inhibitor) was included in the bath solution throughout the experiments. After equilibration, the aortic ring was challenged with phenylephrine (1 μM) to establish a sustained contraction (~20 mN) before fomononetin and other drugs (genistein, diadzein and biochanin A) (0.1 μM - 100 μM) were added cumulatively to the organ baths. A completed (i.e. 100 %) relaxation was considered when the phenylephrine-induced active tone returned to basal level.

The integrity of the functional endothelium was confirmed by acetylcholine (10 μM)-induced relaxation (> 85%) on high K^+ (30 mM) pre-constricted aortic preparations. In some studies, the successful removal of endothelium (by mechanical rubbing the lumen of the aorta with a blunted forceps) was considered when the acetylcholine (10 μM)-induced relaxation was < 5%. In studies with manoeuvres such as endothelium denudation and administration of L-NAME, concentration of phenylephrine added was adjusted (0.35 - 0.6 μM) so as to achieve a comparable magnitude of contractile tone (~20 mN) as observed in endothelium-intact preparations in response to 1 μM phenylephrine challenge. Inhibitors employed in this study were added 30 min before phenylephrine administration and present throughout the experiments.

The Animal Experimentation Ethics Committee of The Chinese University of Hong Kong (HKSAR, PR of China) approved all experiments performed in this study (approval no: 04/054/MIS). The recommendations from the Declaration of Helsinki and the internationally accepted principles for the use of experimental animals were adhered to. Every effort was made to limit animal suffering and to limit the number of animals used in these experiments.

2.3. Incubation of aortic rings

To evaluate the *in vitro* effect of formononetin on isolated aorta, the aortas (thoracic and abdominal) were excised and cleared of all adherent tissues in ice-cold

phosphate buffered saline (pH 7.4) under sterile conditions. The isolated aortas were placed in ice-cold Krebs' solution, washed three times in phosphate buffered saline, and cut into segments of 1 cm long using a scalpel. Four aortic rings were obtained from each rat. The aortic rings were incubated in 24-well plate with physiological salt solution (2 ml per well) in the presence of 1 μM acetylcholine (plus 1 μM neostigmine, an anti-cholinesterase), formononetin (10 μM, 100 μM and 1 mM) or saline (served as control) under an atmosphere of 5% CO_2 and 95% O_2 at 37 °C. After 2 hr incubation, each segment was blotted dry and weighed, and immediately stored at -80 °C for NOS activity assay or in liquid nitrogen for RNA and protein extraction.

2.4. NO content in culture medium and NOS activity of aortic rings

After 2 hr incubation, the medium (2 ml) of each well was collected in micro-centrifuge tubes, and dried by vacuum freeze-drying. The pellets collected were re-dissolved in distilled water (300 μl). Nitric oxide content present in the medium was determined according to the Griess methods [21], and nitrite concentrations were determined at 550 nm using the standard solutions of sodium nitrite.

The NOS activity of isolated aorta was measured as described previously [22]. The frozen sample of aorta (weight = 0.03 – 0.04 g) was homogenized in ice-cold saline (final concentration 10% (w/v)) and centrifuged (3000 rpm, 10 min). The supernatant collected was used for the determinations of total NOS (tNOS) and inducible NOS (iNOS) activities using kits following the instructions of manufactory.

The protein content was evaluated according to Bradford methods. Endothelial NOS (eNOS) activity was estimated (to measure the color change of reagent at 530 nm) as the difference between tNOS and iNOS. It is based on the fact that eNOS is a Ca^{2+}-dependent isoform whereas iNOS is a Ca^{2+}-independent isoform. Thus, the activity of iNOS was estimated in the presence of eNOS inhibitor (L-NAME) plus EGTA (2 mM, a Ca^{2+} chelator) [22]. The NOS activities measured were expressed in U/mg protein.

2.5. Isolation and Quantification of mRNA

To determine the gene expression levels, total RNA was isolated from aorta using TRIzol reagent (Molecular Research Center, Inc., USA). The RevertAid 1st Strand cDNA synthesis system for RT-PCR (MBI Fermentas) with oligo$(dT)_{18}$ was used to obtain the cDNA (in 20 μl of RT-reaction mixture). Total reaction mixture (20 μl) containing 3 μl of the RT-reaction mixture and 0.2 μM of each primer set (Table 1) was prepared to determine eNOS mRNA expression using real time RT-PCR procedures [ABI PRISM 7000 Sequence Detection System with qPCR SuperMix kit (Invitrogen)]. Expression levels of cDNA were compared to internal standard glyceraldehydes 3-phosphate dehydrogenase (GAPDH), a housekeeping gene, to correct for differences in the RNA quantity of samples used. The real-time PCR reaction procedures are as follows: 50 °C for 2 min (UDG incubation), 95 °C for 10 min (UDG inactivation and DNA polymerase activation), then 40 PCR cycles which

consisted of denaturation for 15 s at 95 °C, annealing and extension for 60 s at 53 °C. The second derivative maximum (log linear phase) for each amplification curve was determined using the GAPDH standard curve to calculate the amount of product generated. Each real-time RT-PCR reaction was performed in triplicate. The expression levels of mRNA were expressed as the ratios of mRNA expression of NOS enzyme to that of GAPDH.

2.6. Western immunoblot analysis of phospho—eNOS and eNOS protein expression on thoracic aortas

To determine the protein expression levels, thoracic aortas from different treatment groups were homogenized in the presence of protease inhibitors to obtain extracts of proteins. Protein concentrations were determined using BCA™ protein assay kit (Pierce, USA). Samples (25 μg of protein per lane) were loaded onto a 10% SDS-polyacrylamide electrophoresis gel. After electrophoresis (180V, 60 min), the separated proteins were transferred (12 mA, 45 min) to polyvinylidene difluoride membrane (PerkinElmer™ Life Sciences, USA). Non-specific sites were blocked with 5% non-fat dry milk for 120 min, and the blots were then incubated with anti-phospho-eNOS^{Ser1177} antibody (Upstate, USA) overnight at 4 °C. Anti-rabbit HRP-conjugated IgG, 1:1,000 (Bio-Rad, USA) was used to detect the binding of its correspondent antibody. Membranes were stripped and re-blotted with anti-eNOS antibody, 1:10,000 (Sigma-Aldrich, USA) to verify an equal loading of protein in

each lane. The protein expression was detected with Western Lightning Chemiluminescence Reagent Plus (PerkinElmer Life Sciences, USA) and quantified using Scion Image (version 1.64) programme (NIH, USA).

2.7. Isolation of aortic smooth muscle cells and patch-clamp electrophysiology

Rat aorta (endothelium denuded) smooth muscle cells were enzymatically dissociated (using collagenase and papain) with methods as reported previously by our group [23–25] for single cell patch-clamp electrophysiology experiments. Solutions (external bathing solutions and pipette solutions) and voltage protocols used for whole-cell recordings of BK_{Ca} and K_{ATP} channels were similar to our previous reports [24,25].

2.8. Statistical analysis

Data are expressed as means ± S.E.M., and n denotes the number of replications for each data point. Relaxation was expressed as the percentage of the contraction elicited by phenylephrine. GraphPad Prism 4.02 (San Diego, California, USA) was used to fit sigmoidal curves and to determine the maximum relaxation effect. After validation of each parameter for homogeneity of variance, differences between groups were assessed by one-way analysis of variance (ANOVA) using SPSS (Version 15) software package for Windows (Chicago, IL, USA). *Post hoc* testing was performed

for inter-group comparisons using the least significance difference (LSD) test.

3. Results

3.1. Relaxation of rat aorta by formononetin

After the phenylephrine (1 μM)-induced contraction reached a sustained/steady-state condition, cumulative application of formononetin (0.1 - 100 μM) caused a concentration-dependent relaxation and a maximum relaxation of 98.50 ± 1.50 % was observed in endothelium-intact preparation. Other phytoestrogens (genistein, daidzein and biochanin A) were evaluated and compared. Similar to formononetin, cumulative administration of these compounds caused a concentration-dependant relaxation of phenylephrine-preconstricted aorta (n = 5 - 6) (Fig. 2). Genistein (≤ 10 μM) elicited a smaller magnitude of relaxation compared to formononetin whereas biochanin A (> 1 μM) induced a similar degree of relaxation as produced by formononetin (Fig. 2). In contrast, daidzein was the least potent one in causing aortic relaxation (Fig. 2). L-NAME (100 μM, a common eNOS inhibitor) and methylene blue (10 μM, an inhibitor of guanylate cyclase), but not 1400W (1 μM, a selective iNOS inhibitor) or propranolol (1 μM, a non-selective β-adrenoceptor blocker), markedly suppressed formononetin-induced relaxation in endothelium-intact preparations (Fig. 3A).

In endothelium-denuded preparations, formononetin (over the same concentration range) elicited a lesser degree of relaxation and a maximum relaxation of 53.28 ± 3.70 % was observed (n = 5 - 6) (Fig. 3B). Methylene blue (10 μM)

attenuated, but not abolished, formononetin-elicited relaxation in endothelium-denuded preparations (n = 5 - 6) (Fig. 3B). However, ICI 182,780 (10 μM, an estrogen receptor antagonist), mifepristone (10 μM, a progesterone receptor antagonist) and propranolol (1 μM, a non-selective β-adrenoceptor antagonist) failed to alter formononetin-induced relaxation observed in both endothelium-intact and -denuded preparations (n = 5 - 6) (data not shown). In time-matched controls, there was no apparent change in phenylephrine-induced active tone of both endothelium-intact and -denuded preparations (data not shown). In endothelium-denuded preparations under resting tension, cumulative application of phenylephrine (10 nM - 10 μM) caused a concentration-dependent contraction and prazosin (10 μM, an α_1-adrenoceptor blocker), but not formononetin (0.01, 0.1 and 1 mM), suppressed phenylephrine-induced contraction (n = 5 - 6) (data not shown).

3.2. Role of K^+ channels activation in formononetin-induced relaxation of endothelium-denuded preparations

In endothelium-denuded preparations, glibenclamide (3 μM, an ATP-sensitive K^+ (K_{ATP}) channel blocker) markedly suppressed formononetin-mediated relaxation (n = 5) (Fig. 4A). A higher concentration of glibenclamide (10 μM) was examined but the phenylephrine-induced active tone was not sustained (n = 6) (data not shown). Thus, effects of glibenclamide (10 μM) on formononetin-elicited relaxation could not be determined accurately. Similar to glibenclamide, iberiotoxin (100 nM, a potent and

highly selective Ca^{2+}-activated K^+ (BK_{Ca}) channel blocker) markedly reduced the magnitude of formononetin-induced relaxation in endothelium-denuded preparations (n = 5) (Fig. 4B). A combination of glibenclamide (3 μM) plus iberiotoxin (100 nM) completely abolished formononetin-induced relaxation in endothelium-denuded preparations (n = 5) (Fig. 4C). Application of glibenclamide, iberiotoxin and a combination of glibenclamide plus iberiotoxin did not alter the resting tension of the preparations (n = 5 - 6) (data not shown).

In single aortic smooth muscle cells, formononetin (10 μM and 100 μM) activated, in a concentration-dependent manner, the basal K_{ATP} channel openings (n = 6) (Fig. 5A) which was eradicated by glibenclamide (3 μM) (n = 6) (Fig. 5A). In addition, formononetin (10 μM, 100 μM and 1 mM) activated, in a concentration-dependent manner, the basal BK_{Ca} channels (n = 6) (Fig. 5B) which was sensitive to iberiotoxin (100 nM) (n = 6) (Fig. 5B).

3.4. Determination of nitric oxide production

To further investigate the effects of formononetin on NO release from aortic endothelial cells, isolated aortic rings were treated with different concentrations of formononetin, and acetylcholine (1 μM) was used as the reference for comparison. Before the addition of acetylcholine, no detectable levels of NO could be measured even after 2-hr incubation. Immediately after acetylcholine (1 μM) (with neostigmine (10 μM, an inhibitor of cholinesterase [26])) was added, NO production was increased

and it reached 88.8 ± 6.44 μM NO per g of aortic ring (Control in Fig. 6) at the end of the incubation period. Similar to acetylcholine, formononetin (10 μM, 100 μM and 1 mM) caused a significant and concentration-dependant increase in NO release. The increase in NO production caused by formononetin (10 μM, 100 μM and 1 mM) were higher than that by acetylcholine (1 μM) by 2.5 % ($P > 0.05$), 14.5 % ($P < 0.05$) and 17.2 % ($P < 0.001$), respectively (n = 4) (Fig. 6).

3.5. Determination of NOS activity

Formononetin (10 μM, 100 μM and 1 mM) markedly increased NOS (presumably eNOS) activity by 31.5% (3.56 ± 0.41 U/mg protein, $P > 0.05$), 65.6% (4.49 ± 0.34 U/mg protein, $P < 0.05$) and 70.8% (4.63 ± 1.28 U/mg protein, $P < 0.05$), respectively (n = 5) (Fig. 7). In the absence of $[Ca^{2+}]_o$ (presumably representing iNOS activity), formononetin has no measurable effects on NOS activity (n = 5) (Fig. 7).

3.6. Determination of eNOS mRNA and protein expression

Formononetin (10 μM, 100 μM and 1 mM) up-regulated eNOS mRNA expression, and a significant increase of eNOS mRNA expression of 1.26 ± 0.17 (92.5 %) and 1.60 ± 0.27 (142.9 %) was observed in the presence of 100 μM and 1 mM formononetin, respectively (n = 5) (Fig. 8A). In addition, formononetin (10 μM, 100 μM and 1 mM) caused a concentration-dependent enhancement of

phospho-eNOS^{Ser1177} protein expression with no apparent change in total eNOS expression (n = 5) (Fig. 8B).

4. Discussion

The present study demonstrates, for the first time, that formononetin (a phytoestrogen) elicited a concentration-dependent relaxation of rat pre-contracted thoracic aortic rings through both endothelium-dependent and -independent mechanisms. Our results (using pharmacological/chemical and molecular biology approaches) illustrate that the endothelium-dependent component of formononetin-induced relaxation, similar to other NO/endothelium-related vasorelaxants, is associated with an increase in NO release which is due to an enhanced eNOS mRNA expression, protein expression of p-eNOS^{Ser1177} (phosphorylated/activated form of eNOS) as well as an increase of eNOS activity. However, our results revealed that acetylcholine managed to cause “a comparable magnitude” of NO release at a much lower concentration (i.e. 1 μM). These results therefore suggest that despite the fact that formononetin caused NO generation from endothelial cells of rat aorta, it is less potent than acetylcholine.

Other phytoestrogens tested in this study (genistein, daidzein and biochanin A) which shared a similar chemical structure to formononetin also elicited a concentration-dependent relaxation of endothelium-intact aorta with a “similar” relaxation profile. It is important to point out that daidzein (a metabolite of formononetin formed *in vivo*) was ~10-fold less potent than formononetin in producing relaxation. The discrepancy in relaxation responses of formononetin and daidzein observed in this study is unknown. It is tempting to speculate that

consumption of herbs e.g. red clove and *Astragalus mongholicus* Bunge which contain a high content of formononetin [27,28] may provide greater beneficial effects (e.g. vasorelaxation) to the cardiovascular systems.

The presence of L-NAME (a common eNOS inhibitor) and methylene blue (a guanylate cyclase inhibitor) mimicked the effects of mechanical removal of endothelium, and an attenuation of relaxation caused by formononetin was observed. In fact, a careful examination of the concentration-response curves of formononetin revealed that methylene blue (10 μM) caused a greater degree of reduction, compared to L-NAME, of formononetin-induced relaxation of endothelium-intact preparations (will be discussed below). Nonetheless, our results clearly demonstrate that formononetin caused a NO-/endothelium-/guanylate cyclase-dependent relaxation. The possible involvement of other NOS isoform such as the inducible NOS (iNOS) was considered. However, our results illustrate that iNOS probably plays no role in the enhanced NO release upon the challenge of formononetin as there was no mRNA and protein expression of iNOS could be detected in our preparations in response to formononetin and acetylcholine challenge (data not shown). In addition, no significant change in NOS activity caused by formononetin was detected in the absence of $[Ca^{2+}]_o$. Thus, our results suggest that the Ca^{2+}-dependent NOS isoform (i.e. eNOS) but not the Ca^{2+}-independent isoform (i.e. iNOS) is responsible for formononetin-induced NO release from endothelial cells. In line with these observations, 1400W (a highly selective iNOS inhibitor) [29] failed to alter formononetin-induced endothelium-dependent relaxation.

In addition to the involvement of NO/eNOS cascade of endothelial cells, the relaxation response of formononetin reduced after the removal of the influence of NO/endothelium (although the magnitude of relaxation was smaller compared to that observed in endothelium-intact preparations) suggesting that formononetin caused an endothelium-independent relaxation. As mentioned above, methylene blue (a soluble guanylate cyclase inhibitor), glibenclamide (a K_{ATP} channel inhibitor) and iberiotoxin (a potent BK_{Ca} channel blocker), but not L-NAME, attenuated formononetin-induced relaxation of endothelium-denuded preparations. Interestingly, a combination of glibenclamide and iberiotoxin abolished formononetin-elicited endothelium-independent relaxation. Thus, our results demonstrate that the endothelium-independent component of formononetin-induced relaxation involved the activation of guanylate cyclase as well as the opening of K_{ATP} and BK_{Ca} channels. To strengthen our conclusion on the type(s) of ion channels involved in formononetin-induced endothelium-independent relaxation, BK_{Ca} and K_{ATP} channels gatings of single cells of aorta were measured. Our novel results reveal that formononetin activated glibenclamide-sensitive K_{ATP} and iberiotoxin-sensitive BK_{Ca} channels which are responsible for the endothelium-independent component of formononetin-induced relaxation.

As illustrated in Fig. 1, formononetin is a phytoestrogen but the failure of ICI 182,780 (10 μM, an estrogen receptors (ERα/ERβ) antagonist) and mifepristone (10 μM, a progesterone receptor antagonist) in altering formononetin-induced vasorelaxation argued against the contribution of estrogen receptor and progesterone

receptor activation. The possible participation of α and β-adrenoceptors on formononetin-induced aortic relaxation was considered. Our results however suggest that neither α_1- nor β_2-adrenoceptors were involved as the presence of prazosin and propranolol did not modify phenylephrine-induced contraction and formononetin-evoked relaxation, respectively.

In conclusion, our novel results demonstrate, for the first time, that formononetin (a phytoestrogen) possesses endothelium-/NO-dependent and endothelium-independent relaxation effects. The endothelium-independent component of formononetin-induced relaxation is associated with the activation of both K_{ATP} and BK_{Ca} channels of the vascular tissues. Thus, our results suggest that consumption of herbs containing formononetin (which is devoid of estrogen/progesterone receptors activation) may provide beneficial effects to the cardiovascular systems of postmenopausal women.

Acknowledgments

We are grateful to assistance provided by technicians of State Key Laboratory of Chinese Medicine and Molecular Pharmacology, Department of Applied Biology and Chemical Technology, Hong Kong Polytechnic University (Hong Kong SAR, PR China). This project was supported by a research grant of the "Shenzhen Virtual University Park", Shenzhen Government (PR China), the Niche Area Research Grant of the Hong Kong Polytechnic University, Direct Grants for Research (The Chinese University of Hong Kong) (Reference no.: 2401149; Project code: 2041231; 2401296), and the RGC Earmarked Grants of Hong Kong SAR (Ref. #: 4107/01M; 4166/02M, project code: 2140565). Mr. Sai-Wang Seto and Ms. Alice L.S. Au are recipients of the post-graduate studentship of the Department of Pharmacology (The Chinese University of Hong Kong, Hong Kong SAR). Proofreading of the manuscript by Mr. Ho-Yeung Lam is also acknowledged.

References

[1] Tham DM, Gardner CD, Haskell WL. Clinical review 97: potential health benefits of dietary phytoestrogens: a review of the clinical, epidemiological, and mechanistic evidence. J Clin Endocrinol Metab 1998;83:2223–35.

[2] Setchell KD, Cassidy A. Dietary isoflavones: biological effects and relevance to human health. J Nutr 1999;129:758S–67S.

[3] Lowe GD, Hormone replacement therapy and cardiovascular disease: increased risks of venous thromboembolism and stroke, and no protection from coronary heart disease. J Intern Med 2004;256:361–74.

[4] Honoré EK, Williams JK, Anthony MS, Clarkson TB. Soy isoflavones enhance coronary vascular reactivity in atherosclerotic female macaques. Fertil Steril 1997;67:148–154.

[5] Catania MA, Crupi A, Firenzuoli F, Parisi A, Sturiale A, Squadrito F, et al. Oral administration of soy extract improves endothelial dysfunction in ovariectomized rats. Planta. Med 2002;68:1142–4.

[6] Squadrito F, Altavilla D, Morabito N, Crisafulli A, D'Anna R, Corrado F, et al. The effect of the phytoestrogen genistein on plasma nitric oxide concentrations, endothelin-1 levels and endothelium dependent vasodilation in postmenopausal women. Atherosclerosis 2002;163:339–47.

[7] Cuevas AM, Irribarra VL, Castillo OA, Yañez MD, Germain AM. Isolated soy protein improves endothelial function in postmenopausal hypercholesterolemic

women. Eur J Clin Nutr 2003;57:889–94.

[8] Yan LP, Chan SW, Chan ASC, Chen SL, Ma XJ, Xu HX. Puerarin decreases serum total cholesterol and enhances thoracic aorta endothelial nitric oxide synthase expression in diet-induced hypercholesterolemic rats. Life Sci 2006;79:324–30.

[9] Cathiroe P. Astragalus roots. In: Roy U, editor. American Herbal Pharmacopoeia and Therapeutic Compendium. CA: Santa Cruz 1999. pp. 1–25.

[10] Wang YP, Li XY, Song CQ, Hu ZB. Effect of astragaloside IV on T, B lymphocyte proliferation and peritoneal macrophage function in mice. Acta Pharmacol Sin 2002;23:263–6.

[11] Lei H, Wang B, Li WP, Yang Y, Zhou AW, Chen MZ. Anti-ageing effect of astragalosides and its mechanism of action. Acta Pharmacol Sin 2003;24:230–4.

[12] Siddiqui MT, Siddiqi M. Hypolipidemic principles of Cicer arietinum: biochanin-A and formononetin. Lipids 1976,11:243–6.

[13] Wang W, Tanaka Y, Han Z, Higuchi CM. Proliferative response of mammary glandular tissue to formononetin. Nutr Cancer 1995;23:131–40.

[14] Mu H, Bai YH, Wang ST, Zhu ZM, Zhang YW. Research on antioxidant effects and estrogenic effect of formononetin from Trifolium pratense (red clover). Phytomedicine 2008; doi:10.1016/j.phymed.2008.07.005

[15] Shi GG, Chen JC, Li ZC, Liu XP. Direct effect of Astragalus membranaceus on coronary artery. Trad Chin. Drug Res Clin Pharmacol 1999;10:38–9.

[16] Zhang BQ, Sun J, Hu SJ, Shan QX, Xia Q. Astragalus membranaceus induced

endothelium-dependent vasomotor effect and its mechanism in rat thoracic aorta. Chin J Pharmacol Toxicol 2005;19:44–8.

[17] Zhang WD, Zhang C, Wang XH, Gao PJ, Zhu DL, Chen H, et al. Astragaloside IV dilates aortic vessels from normal and spontaneously hypertensive rats through endothelium-dependent and endothelium-independent ways. Planta Med 2006;72:621–26.

[18] Tolleson WH, Doerge DR, Churchwell MI, Marques MM, Roberts DW. Metabolism of biochanin A and formononetin by human liver microsomes in vitro. J Agric Food Chem 2002;50:4783–90.

[19] Mishra SK, Abbot SE, Choudhury Z, Cheng M, Khatab N, Maycock NJ, et al. Endothelium-dependent relaxation of rat aorta and main pulmonary artery by the phytoestrogens genisterin and daidzein. Cardiovasc Res 2000;46:539–46.

[20] Hu M, Krausz K, Chen J, Ge X, Li J, Gelboin HL, Gonzalez FJ. Identification of CYP1A2 as the main isoform for the phase I hydroxylated metabolism of genistein and a prodrug converting enzyme of methylated isoflavones. Drug Metab Dispos 2003;31:924–31.

[21] Green LC, Wagner DA, Glogowski J, Skipper L, Wishnok JS, Tannenbaum SR. Analysis of nitrate, nitrite and [15N] nitrate in biological fluids. Anal Biochem 1982;120:131–8.

[22] Tang FT, Qian ZY, Liu PQ, Zheng SG, He SY, Bao LP, et al. Crocetin improves endothelium-dependent relaxation of thoracic aorta in hypercholesterolemic rabbit by increasing eNOS activity. Biochem Pharmacol 2006; 72:558–65.

[23] Au AL, Kwok CC, Lee AT, Kwan YW, Lee MM, Zhang RZ, et al. Activation of iberiotoxin-sensitive, Ca^{2+}-activated K^+ channels of porcine isolated left anterior descending coronary artery by diosgenin. Eur J Pharmacol 2004;502:123–33.

[24] Seto SW, Ho YY, Hui HN, Au AL, Kwan YW. Contribution of glibenclamide-sensitive, ATP-dependent K^+ channel activation to acetophenone analogues-mediated in vitro pulmonary artery relaxation of rat. Life Sci 2006;78:631–9.

[25] Seto SW, Au AL, Lam TY, Chim SS, Lee SM, Wan S, et al. Modulation by simvastatin of iberiotoxin-sensitive, Ca^{2+}-activated K^+ channels of porcine coronary artery smooth muscle cells. Br J Pharmacol 2007;151:987–97.

[26] Iwanaga Y, Miyashita N, Morikawa K, Mizumoto A, Kondo Y, Itoh Z. A novel water-soluble dopamine-2 antagonist with anticholinesterase activity in gastrointestinal motor activity. Comparison with domperidone and neostigmine. Gastroenterology 1990;99:401–8.

[27] Tsao R, Papadopoulos Y, Yang R, Young JC, McRae K. Isoflavone profiles of red clovers and their distribution in different parts harvested at different growing stages. J Agric Food Chem 2006;54:5797–805.

[28] Wang X, Liu T, Li Q, Chen X, Bi K. Simultaneous determination of five isoflavonoids in commercial radix astragali by high performance liquid chromatography. Se Pu 2006;24:486–8.

[29] Garvey EP, Oplinger JA, Furfine ES, Kiff RJ, Laszlo F, Whittle BJ, et al. 1400W is a slow, tight binding, and highly selective inhibitor of inducible nitric-oxide

synthase in vitro and in vivo. J Biol Chem 1997;272:4959–63.

Figure legends

Fig. 1. Chemical structures of formononetin, genistein, daidzein, biochanin A, estrogen and progesterone.

Fig. 2. Cumulative concentration-response curves of formononetin (◯), genistein (▼), daidzein (■) and biochanin A (◆) in phenylephrine (1 μM) pre-contracted rat isolated thoracic aorta (endothelium intact). Data are expressed as means ± S.E.M. (n = 5 - 6).

Fig. 3. (A). Effects of L-NAME (100 μM, ▲), methylene blue (10 μM, ▼), W1400 (1 μM, ◆) and propranolol (1 μM,●) on formononetin-induced relaxation (control, ◯) of phenylephrine pre-contracted rat isolated aorta (endothelium intact). (B) Effects of methylene blue (10 μM, ▲) on formononetin-induced relaxation (control, ◯) of phenylephrine pre-contacted rat isolated aorta (endothelium denuded) (-Endo). Data are expressed as means ± S.E.M. (n = 5 - 6).

Fig. 4. Effects of (A) glibenclamide (3 μM, ●), (B) iberiotoxin (100 nM, ▲) and (C) a combination of glibenclamide (3 μM) plus iberiotoxin (100 nM) (▼) on formononetin-induced relaxation (control, ◯) of phenylephrine pre-contracted rat isolated aorta (endothelium denuded). Data are expressed as means ± S.E.M. (n = 5 - 6). *P < 0.05, **P < 0.01 and ***P < 0.001 compared to controls (◯).

Fig. 5. Effects of formononetin on (A) K_{ATP} channels and (B) BK_{Ca} channels of rat aortic smooth muscle cells. (A) Insets show representative whole-cell K_{ATP} channels elicited with test potentials of -100mV to +40mV (a 20-mV increment for a 600-ms duration, 0.1 Hz) from a holding potential of -60 mV. Calibration bars: 100 pA and 250 ms. Pipette solution contained 100 nM ATP. Summary of the effects of glibencalmide (3 μM), formononetin (10 μM and 100 μM) (with and without glibenclamide 3 μM) on the current-voltage relationship of the whole-cell K_{ATP} channels of rat aortic smooth muscle cells. (B) Insets show representative whole-cell BK_{Ca} channels elicited with test potentials of -80mV to +80mV (a 20-mV increment for a 500-ms duration, 0.1 Hz) from a holding potential of -60 mV. Calibration bars: 400 pA and 250 ms. Pipette solution contained ~400 nM Ca^{2+}. Summary of the effects of iberiotoxin (100 nM), formononetin (10 μM, 100 μM and 1 mM) (with and without iberiotoxin 100 nM) on the current-voltage relationship of the whole-cell BK_{Ca} channels of rat aortic smooth muscle cells. Data are expressed as means ± S.E.M. (n = 6). **P* < 0.05 versus control.

Fig. 6. Determination of nitric oxide (NO) production (μM/g of aorta), *in vitro*, from rat isolated aortas (endothelium intact) in response to acetylcholine (ACh, 1 μM) and formononetin (10 μM, 100 μM, 1 mM). Data are expressed as means ± S.E.M. (n = 4). **P* < 0.05 and ****P* < 0.001 versus ACh.

Fig. 7. Determination of eNOS and iNOS activities of rat isolated aorta (endothelium intact) in response to formononetin (10 μM, 100 μM, 1 mM). Data are expressed as means ± S.E.M. (n = 5). *$P < 0.05$ versus control.

Fig. 8. (A). Effects of formononetin (10 μM, 100 μM, 1 mM) on eNOS mRNA expression (eNOS mRNA/GADPH) of rat isolated aorta (endothelium intact) determined by real time PCR analysis. Data are expressed as means ± S.E.M. (n = 5). *$P < 0.05$ and **$P < 0.01$ versus control (B) Effects of formononetin (10 μM, 100 μM, 1 mM) on phospho-eNOS$^{Ser\ 1177}$ protein and total eNOS protein expression of rat isolated aorta (endothelium intact). Data are expressed as means ± S.E.M. (n = 5). *$P < 0.05$, **$P < 0.01$ and ***$P < 0.001$ versus control.

Table 1

The primer sequences used for real time RT-PCR experiments

Gene name	Forward primer	Reverse primer	Product size (bp)	Accession Number
eNOS	5’GGATTCTGGCAAGACCGATTAC3’	5’GGTGAGGACTTGTCCAAACACT3’	159	U18336
GAPDH	5’TGCACCACCAACTGCTTAG3’	5’AGTGGATGCAGGGATGATGT3’	180	NM017008

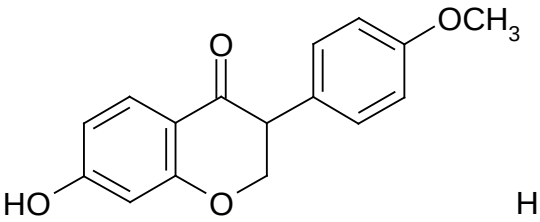

Formononetin

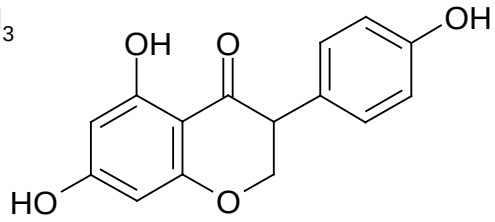

Genistein

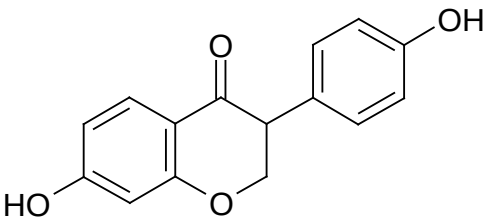

Daidzein

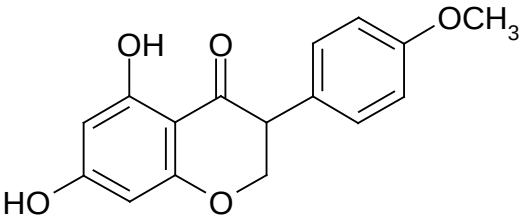

Biochanin A

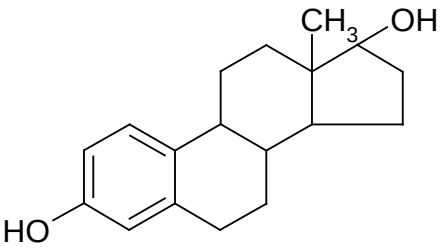

Estrogen

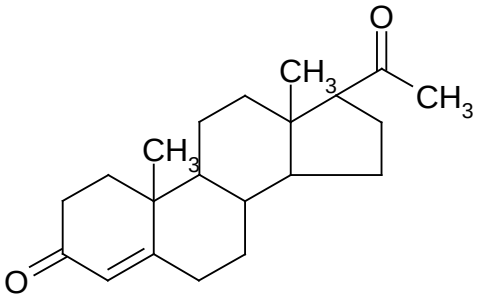

Progesterone

Fig. 1

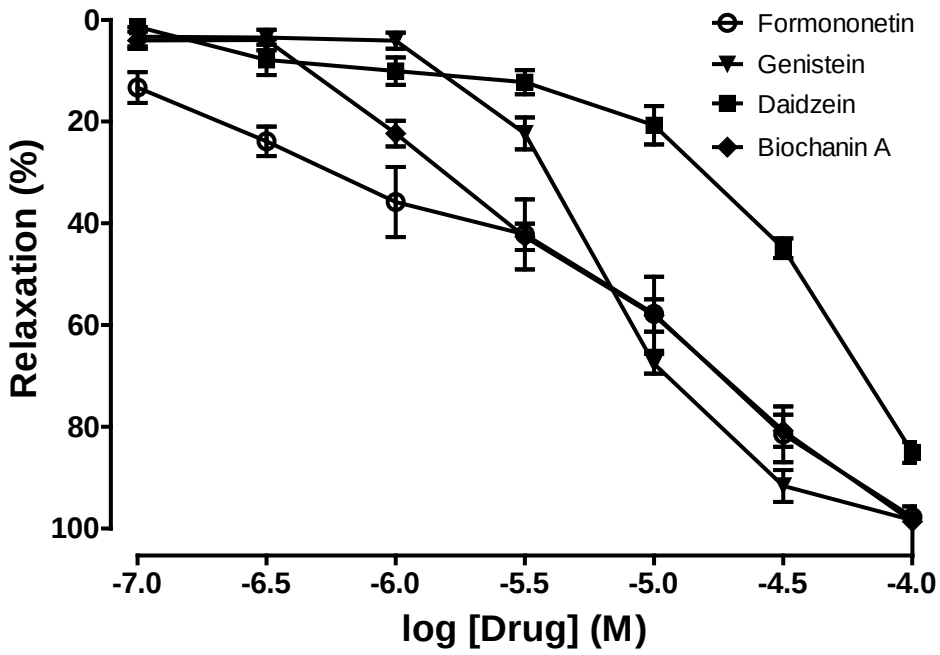
Formononetin
Genistein
Daidzein
Biochanin A
Relaxation (%)
0
20
40
60
80
100
-7.0
-6.5
-6.0
-5.5
-5.0
-4.5
-4.0
log [Drug] (M)

Fig. 2

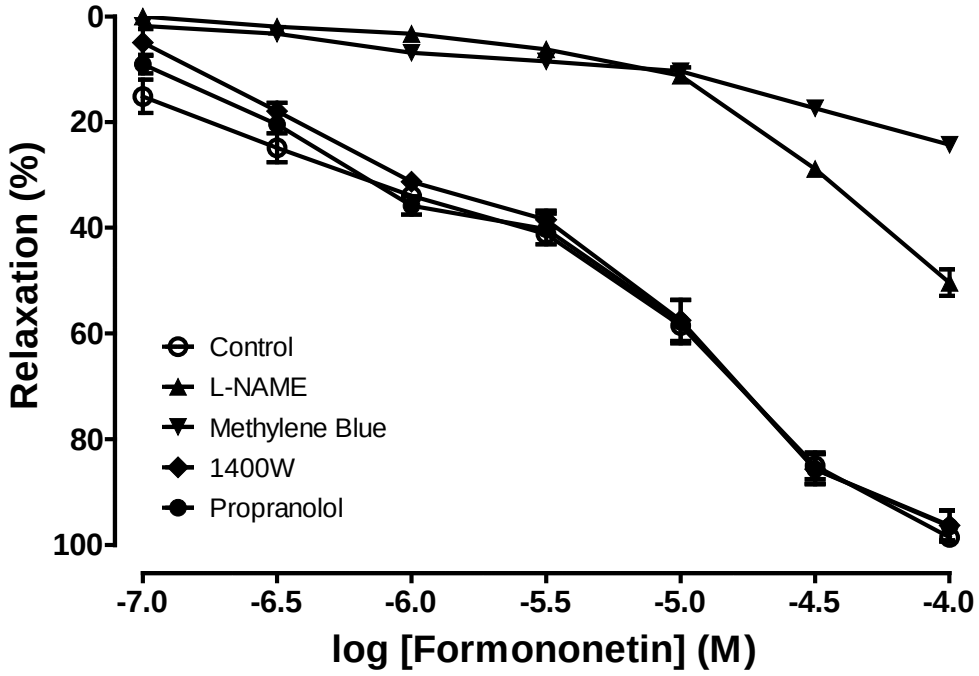
Relaxation (%)
0
20
40
60
80
100
Control
L-NAME
Methylene Blue
1400W
Propranolol
-7.0
-6.5
-6.0
-5.5
-5.0
-4.5
-4.0
log [Formononetin] (M)

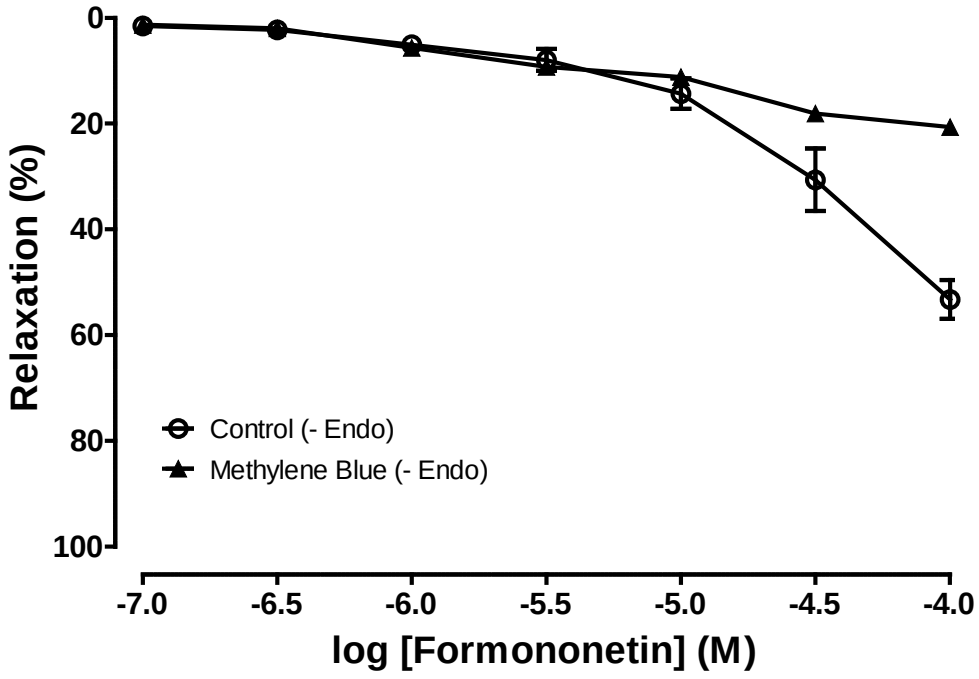
Relaxation (%)
0
20
40
60
80
100
Control (- Endo)
Methylene Blue (- Endo)
-7.0
-6.5
-6.0
-5.5
-5.0
-4.5
-4.0
log [Formononetin] (M)

Fig. 3

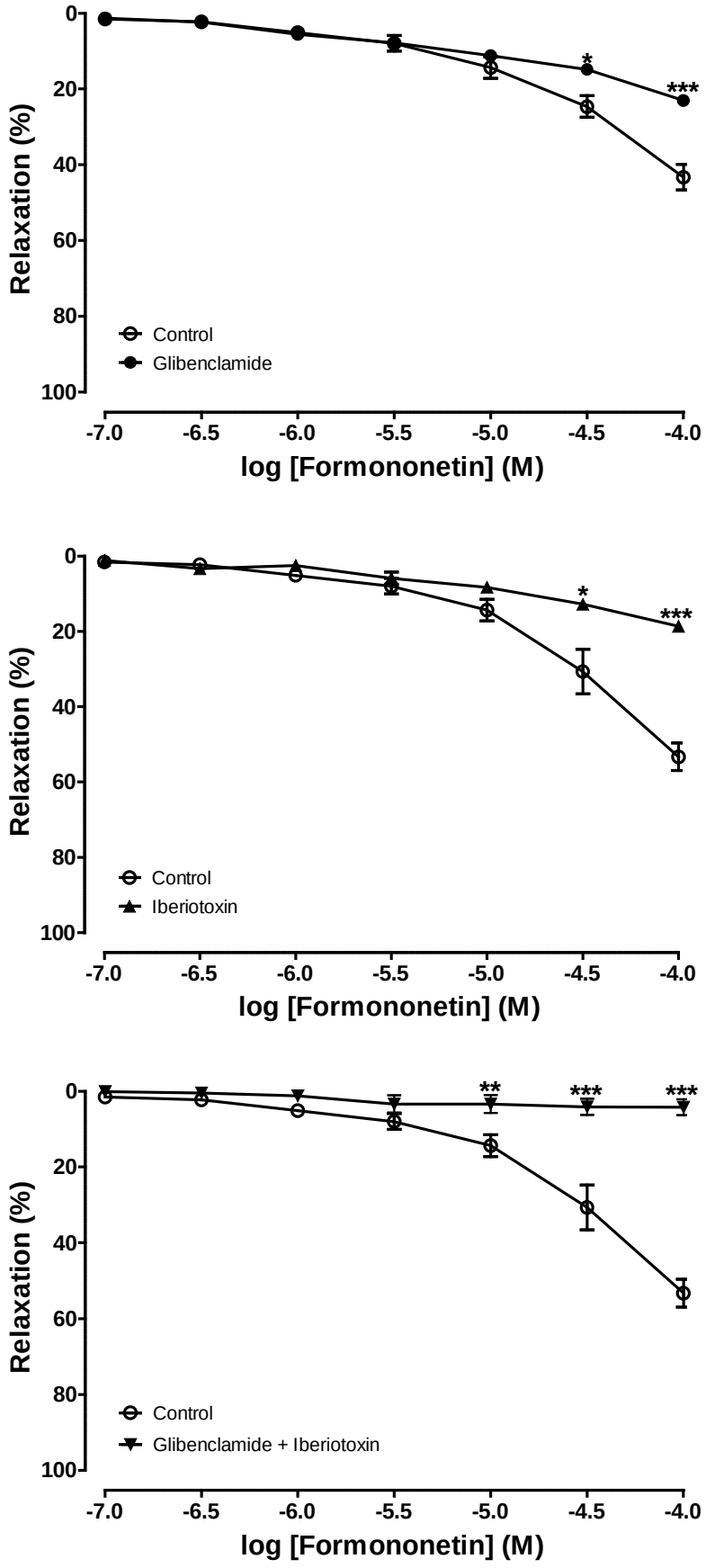
Relaxation (%)
0
20
40
60
80
100
-7.0
-6.5
-6.0
-5.5
-5.0
-4.5
-4.0
log [Formononetin] (M)
Control
Glibenclamide
*
***
Control
Iberiotoxin
*
***
Control
Glibenclamide + Iberiotoxin
**
***
***

Fig. 4

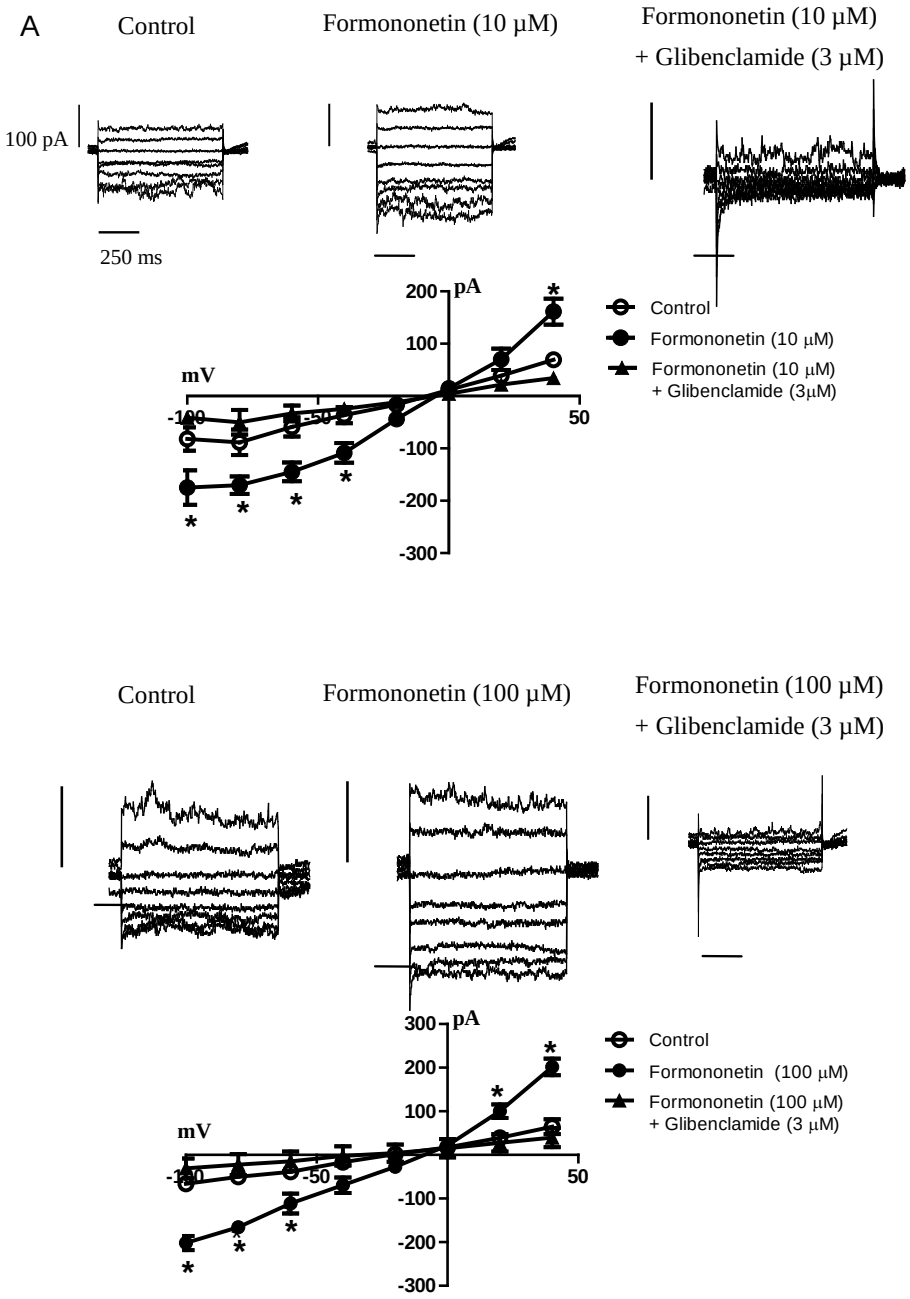
A
Control
Formononetin (10 μM)
Formononetin (10 μM)
+ Glibenclamide (3 μM)
100 pA
250 ms
pA
mV
Control
Formononetin (10 μM)
Formononetin (10 μM)
+ Glibenclamide (3μM)
Control
Formononetin (100 μM)
Formononetin (100 μM)
+ Glibenclamide (3 μM)
pA
mV
Control
Formononetin (100 μM)
Formononetin (100 μM)
+ Glibenclamide (3 μM)

Fig. 5

B

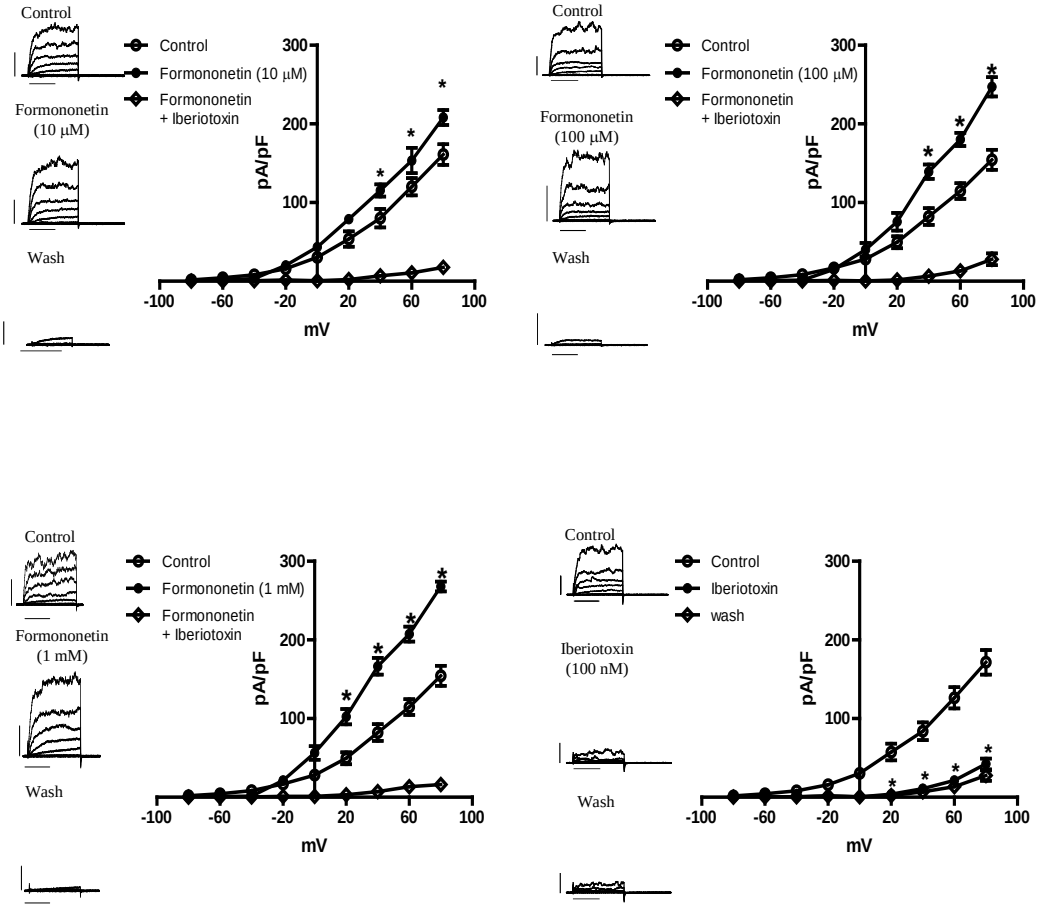
Control
Formononetin
(10 μM)
Wash
Control
Formononetin (10 μM)
Formononetin
+ Iberiotoxin
pA/pF
mV
Control
Formononetin
(100 μM)
Wash
Control
Formononetin (100 μM)
Formononetin
+ Iberiotoxin
pA/pF
mV
Control
Formononetin
(1 mM)
Wash
Control
Formononetin (1 mM)
Formononetin
+ Iberiotoxin
pA/pF
mV
Control
Iberiotoxin
(100 nM)
Wash
Control
Iberiotoxin
wash
pA/pF
mV

Fig. 5

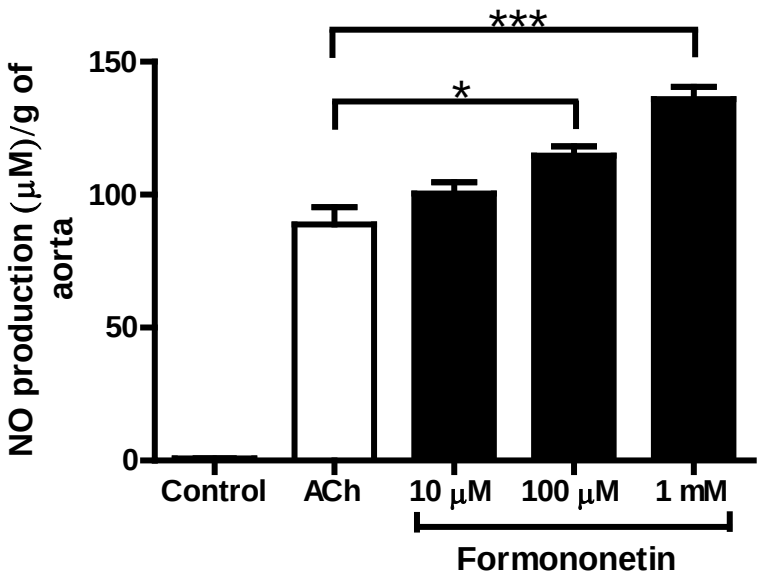
***
*
150
100
50
0
NO production (μM)/g of aorta
Control
ACh
10 μM
100 μM
1 mM
Formononetin

Fig. 6

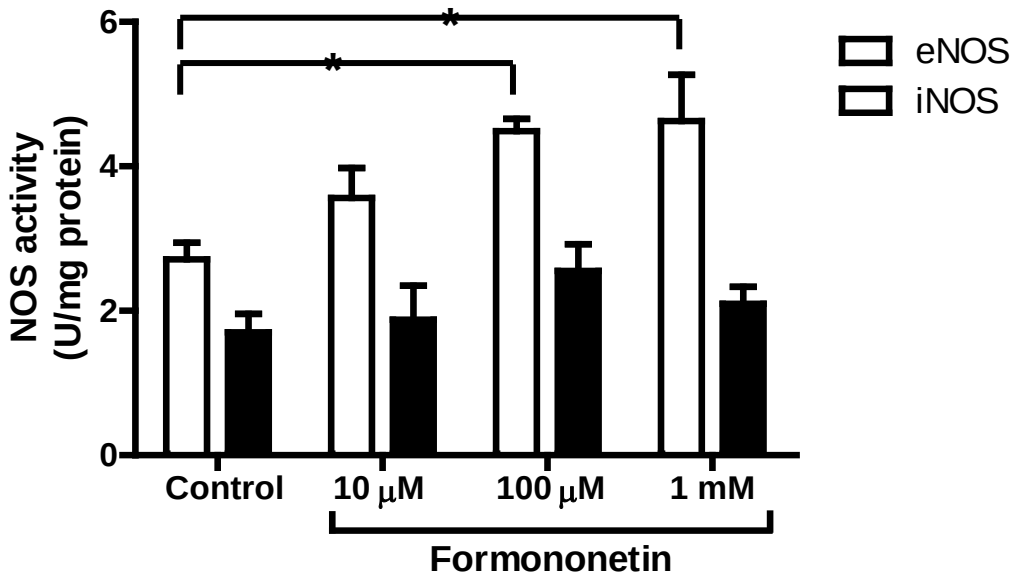
6
4
2
0
NOS activity
(U/mg protein)
*
*
eNOS
iNOS
Control
10 μM
100 μM
1 mM
Formononetin

Fig. 7

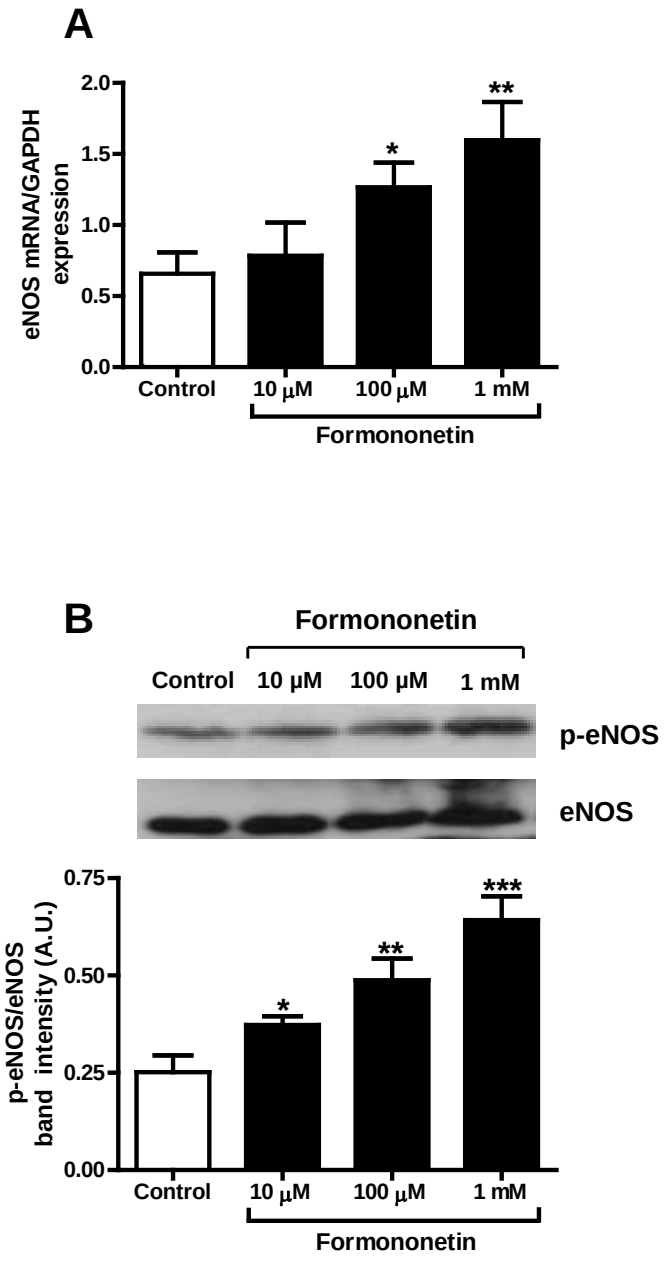
A
eNOS mRNA/GAPDH expression
2.0
1.5
1.0
0.5
0.0
*
**
Control
10 μM
100 μM
1 mM
Formononetin
B
Formononetin
Control
10 μM
100 μM
1 mM
p-eNOS
eNOS
p-eNOS/eNOS band intensity (A.U.)
0.75
0.50
0.25
0.00
*
**
***
Control
10 μM
100 μM
1 mM
Formononetin

Fig. 8